Influence of Driver Stature and Seat Position on Injury Risk in Frontal Car Crashes: A Comparative Analysis of Field Data and Human Body Model Simulations

Martin Östling, Daniel Schmidt, Hanna Jeppsson, Linda Erikson, Thomas Lich

Abstract This study aimed to determine whether a driver's longitudinal seat position influences real-world injury risk and whether a morphed Human Body Model (HBM) can reproduce these risks. Data from 3,847 crash-exposed drivers in the GIDAS database were analysed to examine how stature relates to longitudinal seat position and how longitudinal seat position relates to AIS2+ injury risk. A simulation study evaluated four HBM statures across representative seat positions under 35 km/h and 56 km/h full-frontal crash pulses.

The field data showed no significant effect of longitudinal seat position on injury risk. The morphed SAFER HBMs version 11 reproduced the real-world head injury risks but predicted higher risk for three or more fractured ribs and showed a sensitivity to changed seat position. As this study changed only one factor at a time, while real-world crashes involve many factors changing at once, this sensitivity might be a result of the simplified simulation set-up rather than a proven real-world effect.

For future virtual assessment, it is recommended to start with kinematic-based criteria. Strain-based rib fracture metrics may indicate injury loading but require clearer frameworks for use and interpretation in an assessment context. It is suggested that HBM injury risk validation include comparison to field data across a range of real-world conditions, complementing existing post-mortem human subject-based validation.

Keywords Driver stature, Frontal crash injury risk, Human Body Models, Longitudinal seat position, Real-world crash data.

I. INTRODUCTION

Frontal crashes remain the most frequent crash mode associated with occupant injury in both the US and EU [1-4]. Although advancements in vehicle safety have substantially improved occupant protection in high-severity frontal crashes [5-6], a persistent challenge remains: for belted front-seat occupants, the majority of AIS2+ injuries occur in low- to moderate-severity crashes, primarily due to the high exposure to these events [7-10]. This highlights a critical protection gap and underscores the need to further investigate the factors influencing injury outcomes in these common frontal collision scenarios.

A real-world assessment approach that captures the full range of crash severities, occupant characteristics, and seat position variability, as observed in the field, may provide a representative basis for guiding future restraint system development [11]. Previous investigations examined crash severity and occupant characteristics, showing that injury frequency was dominated by low- to moderate-severity crashes and that injury risk remained largely flat across height and weight distributions [7-10], with elevated risks potentially associated with non-nominal seating postures [12]. However, the influence of a driver's self-selected longitudinal seat position on injury risk remains a potentially critical yet insufficiently investigated factor. Seat longitudinal position defines the occupant's starting distance from the interior surfaces (for example, the steering wheel and the instrument panel) and the restraint system, defining the initial kinematic boundary conditions and influencing when and how the restraints engage during the crash. Therefore, understanding its effect is not a minor detail but fundamental to improving real-world occupant protection.

Driver posture and self-selected seat position are influenced by stature but also by individual preferences. While shorter drivers typically select more forward positions and taller drivers sit farther rearward [13], volunteer studies show wide person-to-person variation, even for drivers of similar stature [14]. Human modelling studies confirm that driving posture depends not only on body size but also on behavioural preferences and car design, contributing to a large variation in longitudinal seat position [15]. Seat position can also be influenced by practical things like rear seat occupancy, luggage, or if a child restraint system is installed.

Field crash data provide mixed evidence regarding how driver stature relates to injury outcome and

M. Östling (e-mail: martin.ostling@autoliv.com; tel: +46 733 614959) is a System Development Senior Expert, H. Jeppsson is an Accidentology Manager and L. Eriksson is a CAE specialist, all at Autoliv, Sweden. D. Schmidt is a Research Engineer and T. Lich is an Accident Research Senior Expert, both at Robert Bosch Germany.

self-selected longitudinal seat position. An in-depth UK crash dataset from 1992 to 2001 reported elevated head and lower extremity injury rates for short-stature occupants in frontal impacts [14]. In contrast, newer analyses indicate that injury rates do not differ substantially between drivers below 170 cm and those above 170 cm [16-17], and that confounding factors such as delta-V, driver age, and vehicle segment are more significant [17]. Together, these findings highlight the need to quantify how stature-related differences in longitudinal seat position influence restraint engagement timing, as small variations in initial position might affect the kinematics and thereby the injury risk.

Virtual testing with Human Body Models (HBMs) enables assessment of real-world variability in occupant characteristics, postures, and seating configurations, extending far beyond the capabilities of anthropomorphic test devices (ATDs), which are limited to three discrete sizes for adults [18]. State-of-the-art HBMs support population-based analyses through parameterised morphed models representing a wide range of statures and body shapes [19]. HBMs are therefore an important complement to ATDs when studying the influence of occupant stature and self-selected seat position. Virtual assessment with HBMs can be grouped into three categories: (i) kinematic-based performance metrics capturing occupant motion, belt and airbag interaction, and interaction with interior structures; (ii) kinetic-based measurements, such as section forces and moments; and (iii) local tissue-based strain metrics, such as strain-based rib fracture prediction [18]. Each approach has advantages and disadvantages, and the preferred method depends on the purpose of the assessment and the type of response being evaluated. From 2026, Euro NCAP will, require occupant classification based on adaptive restraint strategies for the driver and front passenger, and HBM simulations are being introduced into the frontal impact assessment framework, with integration planned for 2029 [20-22]. These strategies further strengthen the relevance of HBMs for analysing driver protection across diverse statures and seating positions.

However, despite substantial development, the use of HBMs to predict real-world injury outcomes remains limited, as current models are primarily validated by means of controlled post-mortem human subject (PMHS) tests conducted in a laboratory environment, which may constrain their ability to represent the broad range of real-world occupant kinematics and restraint interactions. Comparisons between stochastic HBM simulations and field data have shown an overprediction of brain injuries and rib fractures and an underprediction of lower extremity injuries [23-24]. This suggests that current models may lack sufficient validation across real-world variations, such as crash configurations, human variability, seating postures, restraint interactions, and vehicle interior geometries. Work on rib modelling and strain-based rib fracture prediction has shown that HBMs can match tissue-level responses in controlled tests, but their accuracy drops as loading and boundary conditions become more complex [25-27]. Together, these studies show the need to assess how consistently HBMs capture real-world injury sensitivities across both global and local injury mechanisms, by including both PMHS tests and field data when validating HBMs responses.

To bridge the gap between real-world injury outcomes and the capabilities of HBMs, this study directly compared the two. First, we quantified how driver stature and longitudinal seat position were related. Then we quantified how longitudinal seat position was related to injury risk. After that we evaluated morphed SAFER HBM version 11 [28-29] by assessing its ability to reproduce these real-world injury risks across a matrix of occupant statures and longitudinal seat positions. Finally, we compared the field data findings with the corresponding HBM predictions, to see where the models aligned with observed injury risks and where they did not. Together, these results provide indications of the current predictive performance of morphed SAFER HBMs version 11 and highlight possible priorities for future model development to enhance its applicability in virtual safety assessment. Although other models have exhibited different predictive injury risks, this approach of comparing field data findings with model predictions should be transferable to any other HBM developed with these applications in mind.

II. METHODS

The study followed a two-stage approach to evaluate how morphed SAFER HBM version 11 reproduced real-world injury risks related to driver stature and longitudinal seat position. First, a field data analysis of the German In-Depth Accident Study (GIDAS) dataset was conducted to establish a quantitative, real-world reference for driver seating behaviour and its relationship with injury risk. Second, based on these findings, a HBM simulation study was performed to assess model predictions across a range of statures, seat positions, and crash severities. The simulation predictions were compared with the field data injury risks.

Stage 1: Field Data Analysis Framework

The field data analysis was designed to provide the empirical basis for the HBM simulation matrix. It was based on a subset of the GIDAS dataset that was reported in Ostling *et al.* [9]: this dataset included belted, front-row occupants (age ≥ 13) in passenger cars (model year ≥ 2002) involved in a single-event frontal crash with another passenger car. For the current study, it was reduced to the subset of drivers (instead of front-row occupants), resulting in a final sample of 3,847 drivers. For each driver, stature, weight, crash severity, and injury severity coded according to the 2015 Abbreviated Injury Scale (AIS) codebook [30], were extracted.

Longitudinal seat position was determined using the GIDAS variables “Distance bulkhead” (SWSITZ) and “Distance seat” (ASVKD), defining the distance from the pedals to the seat’s D-point (Fig. 1) [31]. We are aware of the difficulties measuring both variables after a crash and the associated uncertainties which led the GIDAS consortium to discontinue both variables at the end of 2022. For this analysis, seat position uncertainty is estimated to be within 5 cm due to challenges in repeating the measurement across different vehicles. Cases with a documented change in seat position during or after the crash (GIDAS variable “Seat position changed” SANDERS) were excluded from the dataset (five cases). Longitudinal seat position was investigated separately for the vehicle categories small, mid, large and SUV/Van [8].

The statistical method for the field data analysis involved mostly descriptive methods, including calculations for mean and median. For calculations of confidence intervals, a minimum of n=10 cases per group was required calculated with the approximate method for binomial confidence intervals by Agresti and Coull [32] which tends to overestimate the intervals for small numbers.

The analysis aimed to quantify two key relationships to serve as a baseline for the simulations: (1) the correlation between driver stature and self-selected longitudinal seat position; and (2) the relationship between longitudinal seat position and the risk of sustaining a moderate or more severe injury (MAIS2+).

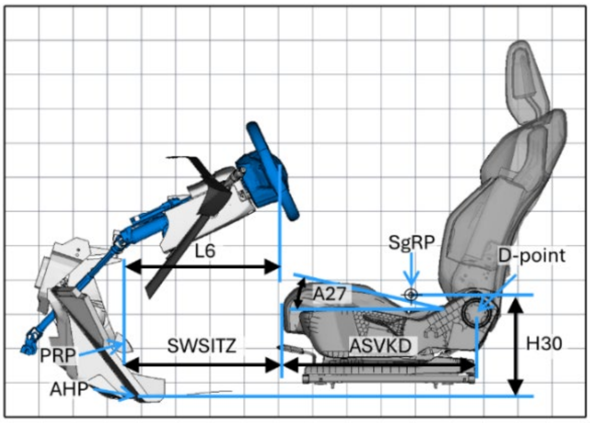

Fig. 1. Frontal Sled FE Model sled model with SgRP, L6, A27, H30, D-point, PRP, and AHP according to SAE J1100 [31], and GIDAS variables SWSITZ and ASVKD used to determined longitudinal seat position.

Stage 2: Human Body Model Simulation Framework

The two key relationships identified in the field data analysis (presented in detail in the Results section) guided the development of a simulation study aimed at assessing the influence of driver stature and self-selected longitudinal seat position on occupant kinematics and injury risk.

Frontal Sled FE Model Description: Geometry, Restraints, and Crash Pulses

Simulations were conducted using an LS-DYNA (version 9.3.0) finite-element (FE) sled model representing a mid-sized European passenger car (Fig 1). The sled model was designed to reflect the restraint system of vehicles represented in the field dataset (model years 2008 ± 5 [9]). Accordingly, the sled model comprised a B-pillar-mounted 3-point belt system with a 2 kN shoulder pretensioner and a 4 kN load limiter (80% of the vehicle fleet was equipped with pretensioner and load limiter [17]), a symmetrical driver airbag (Ø680 mm, Ø32 mm vents), and a collapsible steering column (100 mm stroke at 3 kN), and a deformable steering wheel. The sled model included a detailed FE model of a production seat with seat-back angle (19°), seat height (H30 = 315 mm), seat-cushion angle (A27 = 12.5°) seat-track angle (STA = 0°), and pedal-to-steering-wheel offset (L6 = 511 mm), see Fig.1 [31]. Across all simulations, the seat-back angle, steering-wheel position (L6), and seat-belt height were kept constant. This is consistent with experimental observations, which showed that drivers of shorter stature generally did not adjust seat-back angle, control settings, or belt height, but instead compensated through posture by extending the lower body and flattening the upper leg orientation [16].

A 35 km/h Full Frontal (FF) crash pulse was selected to represent the moderate severity crash conditions most frequently observed in the field where the majority of the AIS2+ injuries occur [8-9]. To evaluate how injury risk changed under more severe loading, a 56 km/h FF crash pulse was also included in the simulation study. Together, these two crash pulses bracket the crash severity range of interest for this study. Restraint activation timings were adjusted for the pulses. In the 35 km/h crash pulse, retractor pretensioner was activated at 18 ms, and the driver airbag at 21 ms. For the 56 km/h pulse, the timings were earlier: retractor pretensioner was activated at 13 ms, and the driver airbag at 16 ms. A visual illustration of how this restraint configuration behaves under the two crash pulses is provided in Appendix B.

Human Body Model and Stature Variants

For the simulation, we used the SAFER HBM version 11, a scalable and omnidirectional HBM developed for biofidelic kinematics and strain-based rib fracture assessment [25-27]. Compared to earlier SAFER HBM versions, it included updates to skeletal structures, soft tissues, and muscular representations, enhancing its capability for tissue-based injury assessment and improving its biofidelity in predicting submarining behaviour [27-28]. The model supported parameterised morphing based on statistical shape models [19]. To reflect the population in the field data, four sizes were selected: a 10th percentile female (F10: 158 cm, 58 kg), a 50th percentile female (F50: 167 cm, 65 kg), a 50th percentile male (M50: 179 cm, 84 kg), and a 90th percentile male (M90: 188 cm, 93 kg), Fig. 2. The percentiles were based on standing stature only. Throughout the study, these models were referred to as F10, F50, M50, and M90. Appendix A explains why these four were chosen and how well they represent the crash-exposed driver population. All morphed SAFER HBMs used a fixed sitting height-to-stature ratio of 0.52.

Seat Positioning Methodology and Driver Posture Definition

To reflect real-world driver variability in the simulation set-ups, the longitudinal seat positions were chosen to span the key trends and variability identified in our field data analysis. To do this we used three distinct methods for defining the longitudinal seat position.

1. Regression-Based: to evaluate stature-driven longitudinal seat position, all four SAFER HBMs were positioned according to the regression-based positioning method [13][33]. Accordingly, the longitudinal seat positions for the four HBMs relative to the pedal reference point were 99 cm (F10), 103 cm (F50), 109 cm (M50), and 113 cm (M90), Fig. 2.
2. Fixed-Forward: to evaluate the influence of stature under the same seating condition, all four HBMs were positioned at a fixed longitudinal seat position (99 cm) such that each HBM reached the steering wheel and pedals while maintaining contact with the seat back.
3. Stature-Specific: to evaluate the influence of longitudinal seat position, the mid-size female (F50) and the mid-size male (M50) HBMs were positioned at three longitudinal seat positions representing the distribution observed in the field data for drivers of comparable stature (forward, mid, and rearward). The seat positions are 91 cm, 96 cm, and 102 cm for F50 HBM and 95 cm, 101 cm, and 107 cm for M50 HBM, respectively.

For all simulations, the longitudinal seat position was defined according to methods 1–3 and vertically adjusted for each HBM stature, with F10 uppermost and M90 in the lowest, within a range of 54 mm. The HBMs were positioned on the seat using gravity settling and the hands and feet were positioned to represent a realistic driving posture. Finally, the seat belt was routed for each simulation set-up.

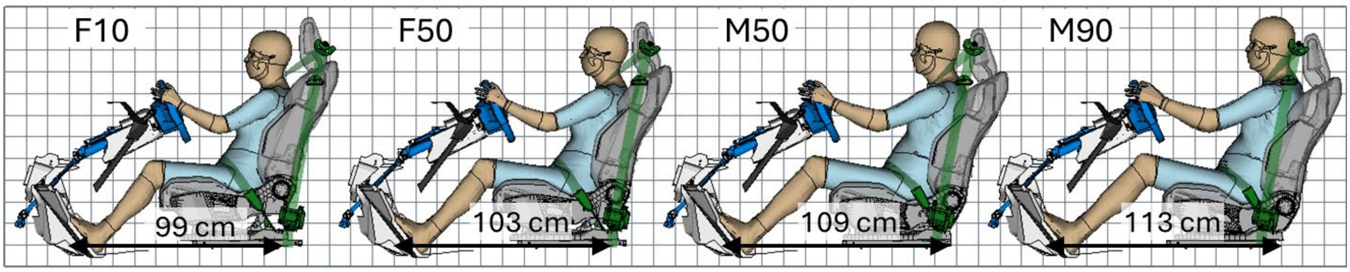

Fig. 2. F10, F50, M50 and M90 HBMs positioned according to methodology 1 (Regression-Based).

Simulation Matrix

The simulation study resulted in 13 unique HBM–longitudinal seat position combinations. Each combination was evaluated under 35 km/h and 56 km/h FF crash pulses, creating a total of 26 simulations.

Comparative Analysis Procedure

First, the overall kinematics were reviewed by checking the head-to-steering wheel distance to identify any strike-through and by examining how the lap belt interacted with the pelvis to detect possible submarining. In addition to these checks, the seat-belt forces (lap and shoulder) and femur forces were evaluated, as these loads provided further insight into injury risk across the different seating positions. Second, head injury risk was assessed using the kinematic criteria HIC15 and DAMAGE together with their corresponding AIS2+ and AIS4+ injury risk functions [34-35]. In addition, head max. x-velocity and head max. y-rotational velocity were evaluated. Third, the risk to sustain three or more fractured ribs, Number of Fractured Ribs ≥3 (NFR3+) was assessed using a probabilistic strain-based method [24][36]. For the NFR3+ risk analysis, the age parameter was set to 45 years to reflect the age of the drivers in the dataset [8-9]. Finally, the simulation results were compared to the injury risks observed in the field data.

III. RESULTS

Field Data: The Real-World Baseline for Stature, Seating Behaviour, and Injury Risk

The analysis of the GIDAS dataset, comprising 3,842 drivers, was performed to establish the quantitative, real-world reference conditions for the HBM simulations. Out of the 3,842 drivers exposed to the crash (=crash-exposed drivers), 205 drivers were injured with a maximum AIS (MAIS) of 2 or more (=injured drivers).The findings are presented in three parts, corresponding to: the selection of HBM anthropometry (stature and weight); the definition of the longitudinal seat position matrix; and the AIS2+ injury risk that the simulations aim to replicate.

Driver Population and Anthropometry

The anthropometric distribution of the driver population was characterised to ensure the selected HBM anthropometries were representative. Fig. 3 plots driver stature against weight for all crash-exposed drivers (grey dots) and the subset of injured drivers, MAIS2+ (red dots). The distribution spanned a wide range of body types with body-mass-indices (BMI) from below 20 kg/m^2 to beyond 35 kg/m^2 and was representative of the German population [8-9]. The overlaid histograms above and right of the main plot for crash-exposed drivers (solid bars) and injured drivers (dashed lines), respectively, showed a high degree of similarity for both stature and weight. This shows that, within this dataset, MAIS2+ injury risk was independent of stature and weight and supporting the selection of HBMs that represent the population's overall anthropometric frequency rather than focusing on a specific, narrowly defined "at-risk" body type.

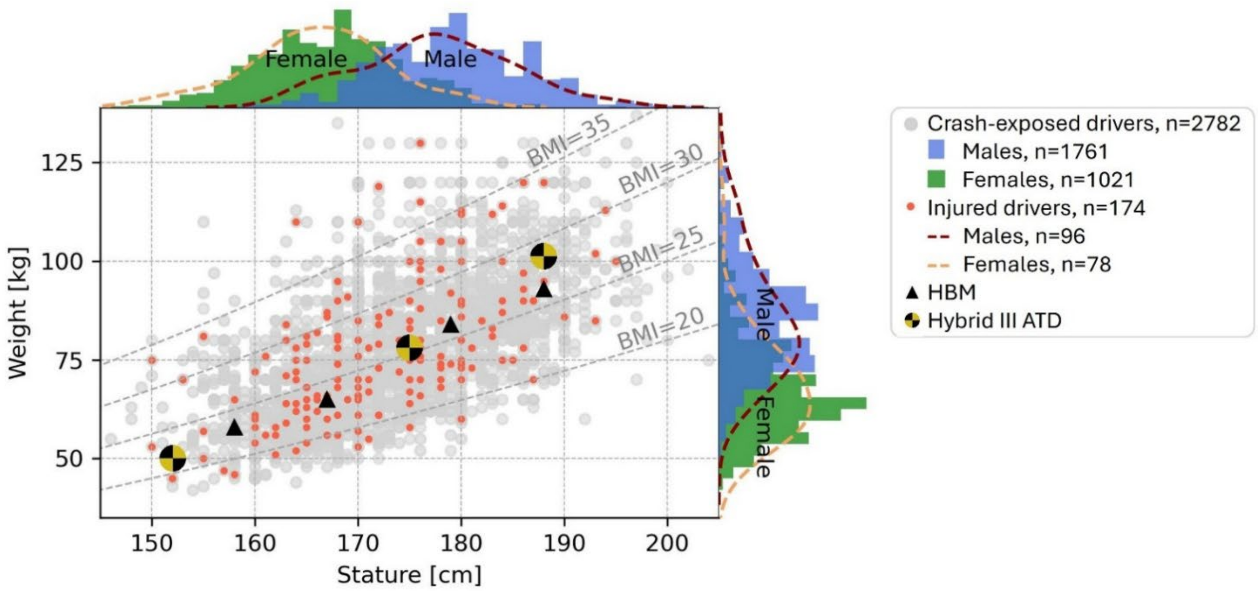

Fig. 3. The main scatter plot shows the distribution of crash-exposed drivers with known stature and weight in grey dots (n=2,782). MAIS2+ injured drivers are marked with red dots (n=174). HBMs used in this study are marked with black triangles. Hybrid III 5% female, 50% male, and 95% male are shown for reference. The histograms of crash-exposed drivers, males (blue) and females (green), show the distribution of stature (top) and weight (right); MAIS2+ injured drivers are shown in dashed lines.

Driver Seat Position as a Function of Stature

The relationship between driver stature and their self-selected seat position was investigated to inform the simulation matrix. The field data gives insights into two simulation parameters: the seat-back angle and the longitudinal seat position. For the seat-back angle, the field data confirms the parametrization of the simulations (19°) as 95% of all driver seats with known seat-back angles are below 20°. Regarding the longitudinal seat position, for the vast majority of cases, it is unknown if the seat was in its original longitudinal position: out of the 2,326 cases with a known seat position, only 708 cases were marked as "seat unchanged" (GIDAS variable SANDERS=2) while for 1,618 cases, the variable was either not coded (before 2008) or marked as unknown. A statistical comparison of the seat position for both groups (seat unchanged vs unknown if seat was changed) did not indicate a systematic alteration of seats for cases with known seat positions: the histograms follow the same distributions and the mean of the longitudinal seat position for both groups differ by 2.5 cm (seat unchanged: 99.4 cm vs not known if seat was changed: 101.9 cm). That gave us the confidence to include the 1,618 cases of "unknown if seat was changed" into the analysis.

Figure 4 reveals two contrasting and equally important characteristics of driver seating behaviour. On one hand, it shows substantial person-to-person variation, reflecting individual preferences; for any given stature, a wide range of seat positions is observed, irrespective of the vehicle category. On the other hand, shorter drivers tend to sit more forward and taller drivers tend to sit more rearward (see also Appendix C, especially tables C1 and C2). This dual finding – an average trend combined with large individual variability – directly motivated the comprehensive design of the 13 HBM–seat position combinations. The simulation matrix was designed not only to evaluate longitudinal seat positions along this central linear trend but also to explore the effects of forward and rearward deviations from that average, reflecting the full spectrum of real-world driver behaviour.

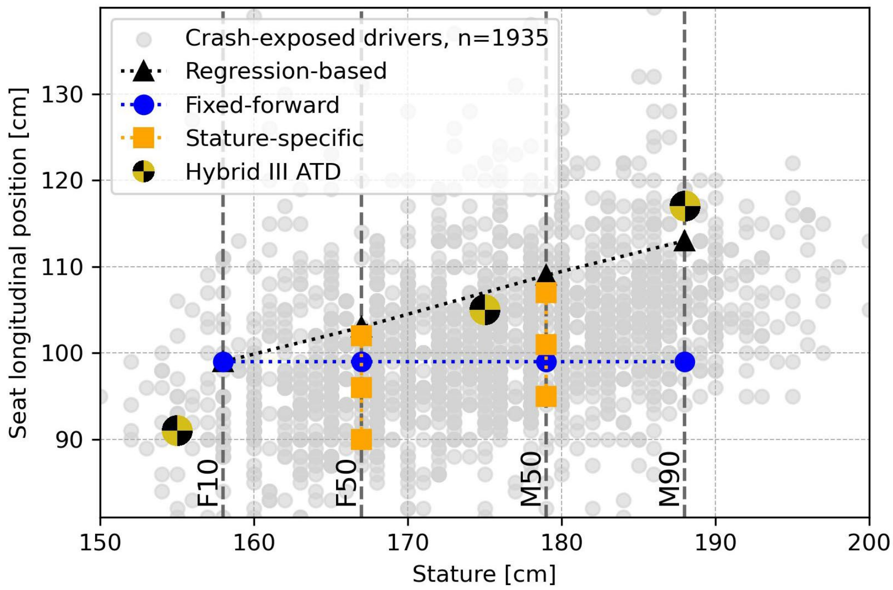

Fig. 4. Stature and longitudinal seat position show a large individual spread with generally more rearward positions for drivers of taller stature. The three different methods for HBM longitudinal seat position are marked with symbols connected for visual guidance with dotted lines. Again, HIII ATDs are marked for reference.

Injury risk as a function of seat position

After evaluating the longitudinal seat position and how it correlates to driver stature, we investigated whether longitudinal seat position correlated with injury outcome. The key finding from this analysis is the lack of a statistically significant difference between the two distributions shown in Fig. 5: the distribution for injured drivers (red bars) closely mirrors the shape of the histogram for all crash-exposed drivers (green bars), and this similarity holds true for both moderate crash severity (Energy Equivalent Speed (EES) 26–40 km/h) and high crash severity (EES > 40 km/h). For both severities, the number of cases including injured drivers (n=47 and n=29 for moderate and severe crashes, respectively) is quite small resulting in large statistical uncertainties.

The injury risk, defined as the ratio between injured and crash-exposed drivers, as a function of the seat position, grouped in 10 cm seat position bins (black dots), was calculated for groups with more than 10 crash-exposed drivers. The average overall MAIS2+ injury risk, represented by the dotted lines in Fig. 5, is 10.5% for moderate crash severity (EES 26–40 km/h); with AIS2+ injury risk for the head of 3.4% and injury risk for the thorax of 4.2%. For moderate crash severity, the median EES for injured driver and for exposed drivers is 32 km/h and 30 km/h, respectively. The average overall MAIS2+ injury risk is 31.6% for high crash severity (EES > 40 km/h); with AIS2+ injury risk for the head of 11.8% and injury risk for the thorax of 18.4%. For high crash severity, the median EES for injured driver and exposed drivers is 51 km/h and 47 km/h, respectively. The average age of the exposed drivers was 45 years old in both groups. For all seat positions, the 95% confidence intervals of the injury risk as a function of the seat position (indicated by the vertical error bars) extend across the average injury risk (averaged over all seat positions; black dotted line), indicating that the differences between seat-position-specific injury risk and average injury risk is not statistically significant. Likewise, due to the overlapping confidence intervals for all pairwise combinations, there were no significant differences in injury risk as a function of seat-position.

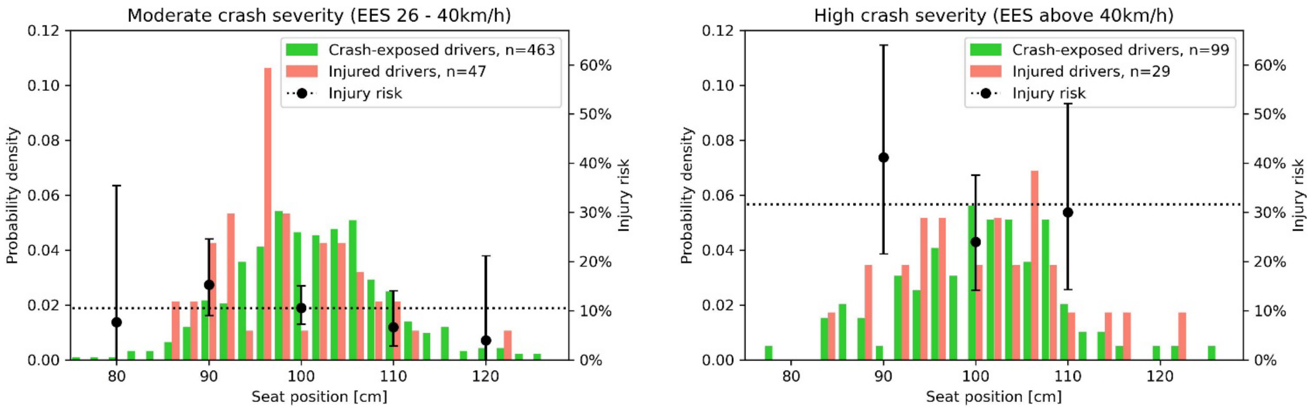

Fig. 5. Comparison of exposed and injured drivers as a function of longitudinal seating position and calculated injury risk. *Left*: moderate crash severity: EES between 26 km/h and 40 km/h. *Right*: high crash severity EES > 40 km/h. Black dotted lines represent the average injury risk. The histograms are scaled for comparability.

In summary, the field data analysis provided the essential empirical foundation for this study. It justified the selection of HBM sizes, informed the detailed HBM longitudinal seat position simulation matrix, and, most importantly, established the real-world injury risk against which the models would be evaluated. It posed a critical biomechanical question: if real-world data did not show a strong link between seat position and injury risk, would the underlying physics and biomechanics – as represented by HBMs – predict one? The following simulation study was designed to answer this question.

Human Body Model Simulation

The following sections describe the results from the 35 km/h and 56 km/h FF crash simulations for all morphed SAFER HBM version 11 sizes, and the longitudinal seat positions defined by methods 1–3, and how these responses compared with the injury risks observed in the real-world dataset. Across all 26 simulations, the HBMs showed stable and consistent behaviour. No airbag strike-through or submarining occurred in any scenario. In every case, the head had more than 5 cm clearance to the steering wheel, and the lap belt remained in contact with the pelvis throughout the crash. Lap-belt forces averaged around 6.5 kN across all runs, with only small differences between the two crash pulses. The variation was roughly ±2 kN, with higher forces in the more rearward seating positions. These changes were offset by the femur forces, which stayed close to 2 kN on average, with about ±1 kN variation depending on the longitudinal seat position. Lower femur forces were seen in the more rearward set-ups. For the shoulder belt, every simulation reached the 4 kN load limiter level, which meant the shoulder-belt force was essentially the same across all configurations.

Head Kinematics and Injury Risk Across Crash Pulses, HBMs and Seat Positions

Head max. x-velocity was slightly higher under the 56 km/h crash pulse compared to the 35 km/h simulations, increasing from 6.9 m/s to 10.2 m/s (average 8.5 m/s) to 8.3 to 12.0 m/s (average 9.7 m/s). A similar trend was seen for head max. y-rotational velocity, 1547 deg./s to 2029 deg./s (average 1740 deg./s) for 35 km/h and 1443 to 2095 (average 1919 deg./s) for 56 km/h, see Fig. 6. The overlapping head kinematic response, despite the different crash severities, is likely due to the restraint system being identical for both pulses, meaning the two crash pulses load the HBMs over different time durations, shorter for the 56 km/h pulse and longer for the 35 km/h pulse.

Compared to the head kinematics, head AIS2+ injury risk based on HIC varied much more between the two crash pulses. It was close to 0% for the 35 km/h crash pulse (3.4% for field data 26–40 km/h EES) and increased to 4.5–24.2 % (average 11.1%) for the 56 km/h crash pulse (11.8% for field data > 40 km/h EES). The highest risk was observed for the M90 in its most rearward seat position and the lowest for M50 in it most forward position. Apart from these two cases, the overall injury risk calculated by HIC was fairly flat across all stature and longitudinal seat positions, staying at around 11% in the 56 km/h crash pulse (see Fig. 6). HIC is driven by head acceleration, therefore the higher injury risk seen in 56 km/h is an expected result [34].

For head injury risk based on DAMAGE, the overall risk was at about the same level for both crash pulses. In the 35 km/h crash pulse, the injury risk ranged from 0.7% to 10.7% (average 3.3%), with the highest risk for the M90 in its most rearward position and the lowest for the same model in its most forward position. In the 56 km/h crash pulse, the injury risk ranged from 0.1% to 5.6% (average 2.8%), with the highest risk for the M50 in its most rearward position, and the lowest for the M50 in its most forward position. For the 35 km/h crash simulations an increased risk for more rearward seat positions could be identified (methods 1 and 3). With the 56 km/h crash pulse, this trend was still present for method 3, but not for method 1 (see Fig. 6). The variation in injury risk across the two pulses (lower risk in 56 km/h) and across different statures and seat positions could not be explained by maximum head velocity or head rotation levels alone. Instead, it reflects the time-dependent behaviour of the DAMAGE metric and how multiple parts of the head kinematics influence the final risk value [37].

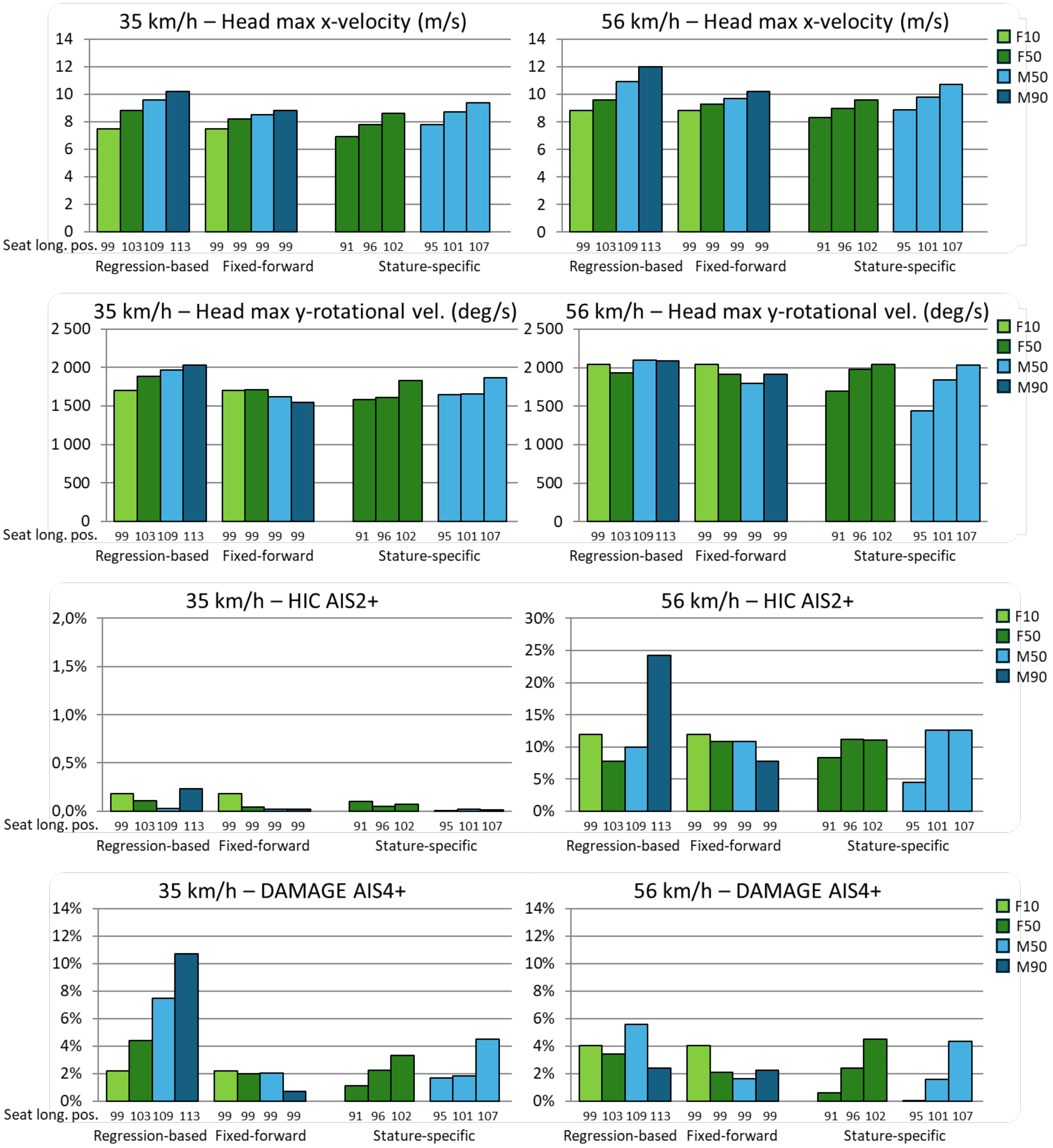

Fig. 6. Comparison of head kinematics (top rows) and had injury risk values (bottom rows) at 35 km/h (*left*) and 56 km/h (*right*) for all HBM statures and longitudinal seat configurations.

Number of Fractured Ribs ≥3 Risks Across Crash Pulses, HBMs and Seat Positions

The predicted risk of getting three or more fractured ribs for a 45-year-old driver (NFR 3+ 45 yr) differed clearly between the two crash pulses. The NFR3+ risk ranged from 8% to 41% (average 22%) for the 35 km/h crash pulse (4.2% AIS2+ thorax injury risk in field data 26–40 km/h EES). The highest values appeared for the F10 in a forward seat position and for the F50 in its most rearward position (Fig. 7). Unlike the field data findings, the morphed SAFER HBMs version 11 showed sensitivity to both stature and longitudinal seat position. The NFR3+ risk was high in almost every simulation, ranging from 43% to 91% (average 79%) for the 56 km/h crash pulse (18.4% AIS2+ thorax injury risk in field data > 40 km/h EES). At this higher crash severity, seat position and stature, almost no effect was observed in the real-world data. Only the F50 showed any noticeable variation, for all other HBMs and longitudinal seat position the risk stayed high regardless of position.

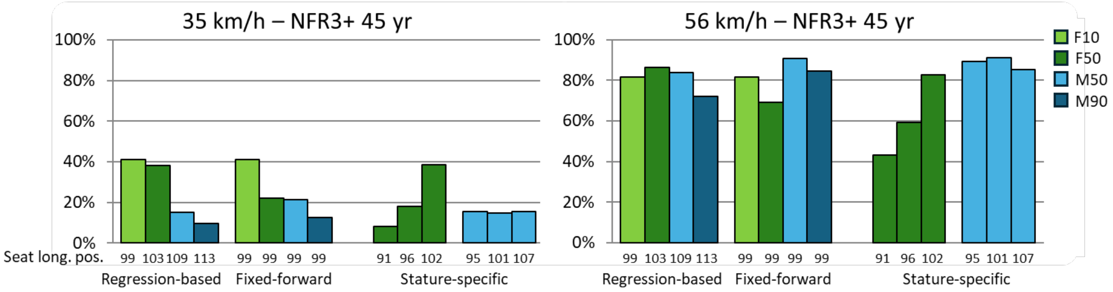

Fig. 7. NFR3+ risk for the 35 km/h (*left*) and 56 km/h (*right*) across all HBM statures and longitudinal seat positionings.

IV. DISCUSSION

This work was initiated to explore how to corroborate injury risk predictions from an HBM with expectations/evidence from field data. As a working example, the specific goal for this study was to assess how well morphed SAFER HBM version 11 represented real-world driver response by comparing its kinematics and injury risk predictions across different driver statures and longitudinal seat positions with calculated injury risks from the GIDAS field crash data. It was shown that neither driver stature nor longitudinal seat position was strongly linked to MAIS2+ injury risk in the field, and that the average MASI2+ injury risk levels were about 10% in moderate severity crashes (26–40 km/h EES) and about 30% in higher severity crashes (> 40 km/h EES). Based on these findings, we evaluated whether the HBM simulations reproduced the same injury risk and compared the model outputs directly with the field data injury risks. The results showed where the model aligned with real-world behaviour most clearly for head injury risk and where it did not, particularly for NFR3+ risk.

For head injury risk, the morphed SAFER HBM version 11 predictions generally followed the injury risks observed in the field crash data, about 3% in 26–40 km/h EES and about 10% in > 40 km/h EES. Injury risk based on HIC increased with crash severity and showed only small differences across stature and longitudinal seat position. In contrast, injury risk based on DAMAGE remained low for both crash pulses but showed limited sensitivity to occupant size or seat position. This indicated that the head kinematics and head injury criteria were reasonably well represented under the two simulated crash pulses. We had no strike-through in the simulations, all cases had more than 5 cm head to steering-wheel clearance.

The situation was different for NFR3+ risk. The morphed SAFER HBM version 11 consistently predicted much higher NFR3+ risk levels than those observed in the field data. Simulations resulted in an average of 22% NFR3+ risk for the 35 km/h crash pulse and in an average of 79% NFR3+ risk for the 56 km/h crash pulse, where filed data show 4% for thorax AIS2+ injury risk for 26–40 km/h EES and 11% for > 40 km/h EES. At 35 km/h, NFR3+ risk showed a sensitivity to stature and seat position, whereas the field data showed no such dependence for MAIS2+ injuries. At 56 km/h, NFR3+ risk was high (often above 80%). This mismatch indicated that the predicted strain-based rib fracture risk in our simulations with the morphed SAFER HBM version 11 did not reproduce the real-world relationship between crash severity, driver size, and seat position and MAIS2+ injury risk.

Taken together, the global kinematics and head injury metrics were reasonably robust, but the strain-based rib fracture risk was more sensitive to the conditions of the simulations. This raised a simple question: was the strong sensitivity seen for the NFR3+ risk just being hidden by noise in the real-world data, or was the simulation study too limited and therefore overstating an effect that was much smaller in reality?

Explanation 1: The "Noisy" Reality and Limitations of Field Data

One interpretation of our findings could be that the calculated high NFR3+ risks from the morphed SAFER HBM version 11 might have been masked within the complexity of real-world crash data. Even a large dataset like GIDAS is highly heterogeneous, spanning many vehicle types and model years, restraint system designs and crash configurations. In contrast, the morphed SAFER HBM version 11 simulations used a single, controlled restraint system and two well-defined crash pulses. Field data also included unavoidable uncertainties of the crash (e.g. crash severity EES based on an estimate and principal direction of force), the driver (e.g. stature, weight, or driver posture at impact), the vehicles (e.g. vehicle size, restraint design, seat-belt force, or airbag performance), and the documented AIS injures (e.g. it is difficult knowing if the true amount of fractured ribs are reported [24]). Together, these factors might have created a wide injury risk distribution that reflected the average of many different crashes rather than a single, well-defined loading condition. As a result, field data were effective for identifying broad trends, such as the increase in injury risk with increased crash severity but were less able to reveal smaller biomechanical sensitivities or to support detailed comparisons of tissue-level injuries like fractured ribs.

Explanation 2: The "Worst Case" Simulation Set-up

A second interpretation could be that the morphed SAFER HBM version 11 overpredicted NFR3+ risk because of the controlled and idealised simulation environment. The prediction of high NFR3+ risk relative to field data might have come from using one sled model and one restraint system design in two relatively severe full-frontal configurations when compared to the field data crashes. This removed many real-world moderating factors, such as softer crash modes like front-to-rear or angled impacts, differences in belt loading between vehicles and adaptive restraint behaviour and created a repeatable *worst case* loading scenario that might have increased the NFR3+ risk. The morphed SAFER HBM version 11 might therefore have been accurately predicting the physics within this idealised set-up, but that set-up did not fully represent the variety and complexity of loading conditions seen across the field data.

Implications for Virtual Testing and the Integration of HBMs in Safety Assessment

Regardless of the exact cause, the discrepancy between morphed SAFER HBM version 11-predicted NRF3+ risk and field data MAIS2+ injury risk has important implications for the use of HBMs in virtual safety assessment. As HBMs become more integrated into frameworks such as Euro NCAP [22], there is a risk that design decisions could be guided by model sensitivities that do not reflect real-world injury risks. If a model shows a strong dependence on a parameter such as longitudinal seat position that is not associated with elevated injury risk in the field, optimising restraint systems around that sensitivity may not yield meaningful real-world safety improvements and could even shift design efforts away from more critical factors.

Study Limitations and Recommendations for Future Research

This study has several limitations. The simulations were performed with only one of the HBMs (morphed SAFER HBM version 11), one vehicle sled model, and two crash pulses. While this controlled set-up helped to isolate specific effects from the seating positions and their selection methods, it means the findings should not be taken too generally. Especially when the field data come with uncertainties, such as the exact crash pulse shape, restraint system design, and seat position accuracy, which makes precise, one-to-one comparisons impossible.

Other limitations from field data worth addressing involve, among others, the limited sample size. Although the entire dataset contains almost 4,000 crash-exposed drivers, a discussion of the injury risk is based of 205 injured drivers. With further classes for comparative analyses, the number might drop to below 50 injured drivers (cf. injury risks in Fig 5). More data could easily add more confidence to our findings. Another limitation is, e.g., the limited knowledge of seat height. While GIDAS, in principle, contains this information, its quantity and quality were insufficient for analysis. For future work, the influence of seating height could be addressed.

Looking ahead, a few clear steps could help to resolve the gaps we identified. A more focused analysis of the field data is needed, preferably by reducing variation and creating a smaller, more uniform subset of the dataset, to enable easier replication in a simulation study. Such a smaller dataset should then be created for different conditions, each of them including a specific crash severity and crash configuration, with injury patterns and injury risks checked for each body region [11]. To support this, Appendix C adds stature-specific seat-position frequencies that, together with the calculated percentiles and population coverage in Appendix A, can help future studies choose seat positions that give the largest real-world coverage. Doing so, one challenge would come from the already low injury risk (around 5%) seen in the field data in crashes up to 40 km/h EES [9][11]. Traditional methods struggle at such low injury probabilities because meaningful improvements to existing injury risk functions would require unrealistically high numbers of PMHS tests. A more practical path is to control the kinematics directly, since these parameters drive the kinematic energy behind many injury mechanisms. Future simulation studies should also include modern adaptive restraint systems to evaluate how they might reduce the overall injury risk in low, moderate and severe crashes for occupants of different sizes and in various seat positions. This aligns with Euro NCAP's 2026 direction, which introduces occupant-specific and crash severity-specific restraint concepts, with the purpose of driving down the overall injury risk, an approach that matches well with the needs highlighted in this study.

V. CONCLUSIONS

The field data showed that drivers choose a large variety of longitudinal seat positions, based on personal preferences and not only according to their stature, but these differences did not show any significant effect on their injury risk in single-event frontal crashes with another car.

The morphed SAFER HBM version 11 simulations matched the real-world head injury risks, showing similar levels and only small effects from height or seat position. The simulations, however, predicted much higher NFR3+ risks and showed a sensitivity to seat position, which was not seen in the field data. Because this study changed only one variable at a time, while real crashes include many factors changing at once, a direct comparison to real-world injury outcomes is not possible. A better way forward is to use stochastic simulations, where many factors vary together to reflect the full range of real-world conditions. Even so, the model likely captured the key kinematic behaviour well, meaning future virtual assessments can rely on HBMs for motion across different sizes and seat positions. The high NFR3+ predictions remain an important challenge, and more work is needed to understand how these model outputs should guide decisions in rating or regulatory use.

VI. REFERENCES

[1] Craig, M. J., Liu, C., Zhang, F., Enriquez, J. (2023) Sex-based differences in odds of motor vehicle crash injury outcomes (Report No. DOT HS 813 513). National Highway Traffic Safety Administration.

[2] Noh, E. Y., Atwood, J. R. E., Lee, E., Craig, M. J. (2022) Female crash fatality risk relative to males for similar physical impacts (Report No. DOT HS 813 358). National Highway Traffic Safety Administration.

[3] Odriozola, M. de, Vilchez, S., Östling, M., D'Addetta, G. A., Merdivan, D. (2021). SAFE-UP Deliverable D4.1: Use case definition. https://static1.squarespace.com/static/5efaed43294db25b18168717/t/64909b1c1f1bd013e622b2c1/1687198530410/SAFE-UP_D4.1_USE+CASE+DEFINITION_.pdf. Accessed 23 March 2026.

[4] Edwards, M. J., Hynd D., Thompson A., Carroll J., Visvikis C. (2009) Technical Assistance and Economic Analysis in the Field of Legislation Pertinent to the Issue of Automotive Safety: Provision of information and services on the subject of the tests, procedures and benefits of the requirements for the development of legislation on Frontal Impact Protection. Transport Research Laboratory.

[5] Kullgren, A., Axelsson, A., Stigson, H., Ydenius, A. (2019) Developments in Car Crash Safety and Comparisons Between Results From Euro NCAP Tests and Real-World Crashes. The 26th International Technical Conference on the Enhanced Safety of Vehicles (ESV), 2019, Eindhoven, Netherlands.

[6] Hoye, A. (2019) Vehicle registration year, age, and weight - Untangling the effects on crash risk. *Accident Analysis & Prevention*, **123**: pp. 1–11.

[7] Forman, J. L., Östling, M., Mroz, K., Lubbe, N. (2023) Potential Injury Criteria for Collisions with Heavy Goods Vehicles. The 27th International Technical Conference on the Enhanced Safety of Vehicles Conference, 2023, Yokohama, Japan,. Paper Number 23-0334.

[8] Ostling, M., Jeppsson, H., Forman, J. (2024) Injury Observations in High-exposure, Low-severity Frontal Car Crashes – a GIDAS Investigation. *Proceedings of the IRCOBI Conference*, 2024, Stockholm, Sweden.

[9] Ostling, M., Jeppsson, H., Schindler, R. (2024) Risk of injury and injury pattern with and without an activated airbag for car drivers and front-seat passengers in low-to-moderate severity frontal crashes. The 16th International Symposium and Accompanying Exhibition on Integral Car Safety Systems, Airbag, 2024, Mannheim, Germany.

[10] Forman, J., Jin, R., Östling, M., Jeppsson, H. (2025). Collision, Occupant, and Injury Characteristics in Low- to Moderate-Speed Frontal Collisions – an Examination of US Field Data from 2017 to 2022. *Proceedings of the IRCOBI Conference*, 2025, Vilnius, Lithuania.

[11] Östling, M., Jeppsson, H. (2026). First steps towards a real-world frontal crash assessment matrix: Based on field data exposure and risk with a focus on "exposure severity". Conference presentation, EqOP Frontal Impact and Restraint Requirement Meeting. 3rd meeting TF4 - Transport - Vehicle Regulations - UNECE Wiki. Accessed 23 March 2026.

[12] Hu, J., Lin, Y. S., Boyle, K. J., Reed, M. P., Östling, M. (2025) Identifying Potential Injury Causations and Risk Factors in Moderate Severity Crashes through Parametric Human Modelling. *Proceedings of the IRCOBI Conference*, 2025, Vilnius, Lithuania.

[13] Reed, M. P., Manary, M. A., Flannagan, C. A. C., Schneider, L. W. (2002) A Statistical Method for Predicting Automobile Driving Posture. *Human Factors: The Journal of the Human Factors and Ergonomics Society*, **44**(4): pp. 557–568. https://doi.org/10.1518/0018720024496917.

[14] Welsh, R., Morris, A., Clift, L. (2003) The effect of height on injury outcome for drivers of European passenger cars. *Annual Proceedings – Association for the Advancement of Automotive Medicine*, **47**: pp. 401–416. PMID: 12941238; PMCID: PMC3217531.

[15] Perez Luque, E., Brolin, E., Nurbo, P., Lamb, M., Högberg, D. (2025) A case study of digital human modelling assisted occupant packaging design: Comparing driving posture and position prediction methods. *International Journal of Human Factors and Ergonomics*, **12**(5): pp. 27–57.

[16] Malczyk, A., Müller, I., Eßers, S., Hänsel, M. (2013) Effects of Seating Position of Short Stature Drivers in Frontal Impacts. *Proceedings of the IRCOBI Conference*, 2013, Gothenburg, Sweden.

[17] Liers, H., Rößler, R., Ziegler, J. (2017) Performance of restraint systems in accidents: Does every occupant benefit equally from the measures? *Proceedings of the 25th International Technical Conference on the Enhanced Safety of Vehicles (ESV)*, Detroit, Michigan, United States.

[18] Forman, J., Gepner, B., *et al*. (2026) Strategies for injury prediction with human body models (Paper No. ESV26-175). *Proceedings of the 26th International Technical Conference on the Enhanced Safety of Vehicles (ESV)*, Toronto, Canada.

[19] Hwang, E., Hallman, J., *et al*. (2016) Rapid Development of Diverse Human Body Models for Crash Simulations Through Mesh Morphing. SAE Paper No. 2016-01-1491.

[20] Euro NCAP (2025) *Crash Protection - Frontal Impact Protocol*, Version 1.1, Sept. 2025.

[21] Euro NCAP (2025) *Safe Driving - Occupant Monitoring Protocol*, Version 1.1, Oct. 2025.

[22] Euro NCAP (2025) Human Body Model Simulation for Frontal Impacts. *Technical Bulletin CP 551*, Version 1.1, Dec. 2025.

[23] Ressi, F. and Klug, C. (2024) Stochastic replication of injury risks in frontal collisions with different human body models in a generic vehicle interior. *Proceedings of the IRCOBI Conference*, 2024, Stockholm, Sweden.

[24] Larsson, K.-J., Blennow, A., Iraeus, J., Pipkorn, B., Lubbe, N. (2021) Rib Cortical Bone Fracture Risk as a Function of Age and Rib Strain: Updated Injury Prediction Using Finite Element Human Body Models. *Frontiers in Bioengineering and Biotechnology*, **9**(May 2021): 677768. https://doi.org/10.3389/fbioe.2021.677768.

[25] Iraeus J. and Pipkorn, B. (2019) Development and Validation of a Generic Finite Element Ribcage to be used for Strain-based Fracture Prediction. *Proceedings of the IRCOBI Conference*, 2019, Florence, Italy.

[26] Pipkorn, B., Iraeus, J., Björklund, M., Bunketorp, O., Jakobsson, L. (2019) Multi-Scale Validation of a Rib Fracture Prediction Method for Human Body Models. *Proceedings of the IRCOBI Conference*, 2019, Florence, Italy.

[27] Iraeus, J., Brolin, K., Pipkorn, B. (2020) Generic finite element models of human ribs, developed and validated for stiffness and strain prediction - To be used in rib fracture risk evaluation for the human population in vehicle crashes. *Journal of the Mechanical Behavior of Biomedical Materials*, (106): p. 103742, 2020.

[28] Östh, J., Bohman, K., Jakobsson, L. (2025) Whole-Sequence Rear-End Impact Simulations with an Active Human Body Model. *Proceedings of the IRCOBI Conference*, 2025, Vilnius, Lithuania.

[29] Iraeus, J., Brynskog, E., *et al*. (2024) Development of SAFER HBM v11Report 2024:06, Version 1.0. Chalmers University of Technology, report 2024:06, Gothenburg, Sweden.

[30] Association for the Advancement of Automotive Medicine (AAAM) (2015) Abbreviated Injury Scale v.2015.

[31] SAE International (2009) SAE J1100: Motor Vehicle Dimensions. SAE Standard J1100, Revised Nov. 2009.

[32] Agresti, A., and Coull, B. A. (1998) Approximate is Better than “Exact” for Interval Estimation of Binomial Proportions. The American Statistician, 52(2), 119–126. ttps://doi.org/10.1080/00031305.1998.10480550

[33] Hu, J., Zhang, K., *et al*. (2019) Frontal crash simulations using parametric human models representing a diverse population. *Traffic Injury Prevention*, **20**(sup1): pp. S97–S105.

[34] Craig, M., Parent, D., *et al*. (2020, September) Injury criteria for the THOR 50th male ATD. National Highway Traffic Safety Administration.

[35] Ellway, J., Sandner, V., Eggers, A., Masuda, M. (2023, 21 March) Brain injury calculation (Version 1.0.1; *Technical Bulletin TB 035*). Euro NCAP.

[36] Forman, J. L., Kent, R. W., *et al.* (2012) Predicting rib fracture risk with whole-body finite element models: Development and preliminary evaluation of a probabilistic analytical framework. *Annals of Advances in Automotive Medicine*, **56**: pp. 109–124.

[37] Gabler, L. F., Crandall, J. R., Panzer, M. B. (2018) Development of a second-order system for rapid estimation of maximum brain strain. *Annals of Biomedical Engineering*,**47**(9): pp 1971-1981. doi: 10.1007/s10439-018-02179-9.

[38] Cassola, V. F., Milian, F. M., et al. (2011) Standing adult human phantoms based on 10th, 50th and 90th mass and height percentiles of male and female Caucasian populations. Physics in Medicine & Biology, 56(13): pp. 3749–3772.

VII. APPENDIX

Appendix A: How We Defined the HBM Sizes and Checked That They Represent the Population

In a population, body weight and standing stature are generally not correlated. A person with a 50th percentile body mass can have almost any stature, and someone with an average stature can have any body mass. Many combinations are possible, so we need a reasonable way to define representative adult male and female percentiles. To determine what weights and standing statures HBMs should be morphed to, we used a method introduced by Cassola *et al*. [38]. In short, the method takes weight and stature values from the 10th, 50th, and 90th percentiles of the dataset, and then combines them while keeping the 50th percentile BMI constant. This generates consistent weight–stature pairs across all percentiles. The method included the following steps to define the target values for weight and standing stature combinations for each sex.

1) Calculate standing stature of 10th, 50th, and 90th percentiles based on the female and male datasets.
2) Calculate weight of 10th, 50th, and 90th percentiles for females and males.
3) Calculate BMI by using the calculated percentiles weights by the 50th height.
4) Use the BMI to calculate the 10th, 50th, and 90th percentiles weights for 10th and 90th height.

This resulted in a total of nine target points for females and nine target points for males, Fig. A1.

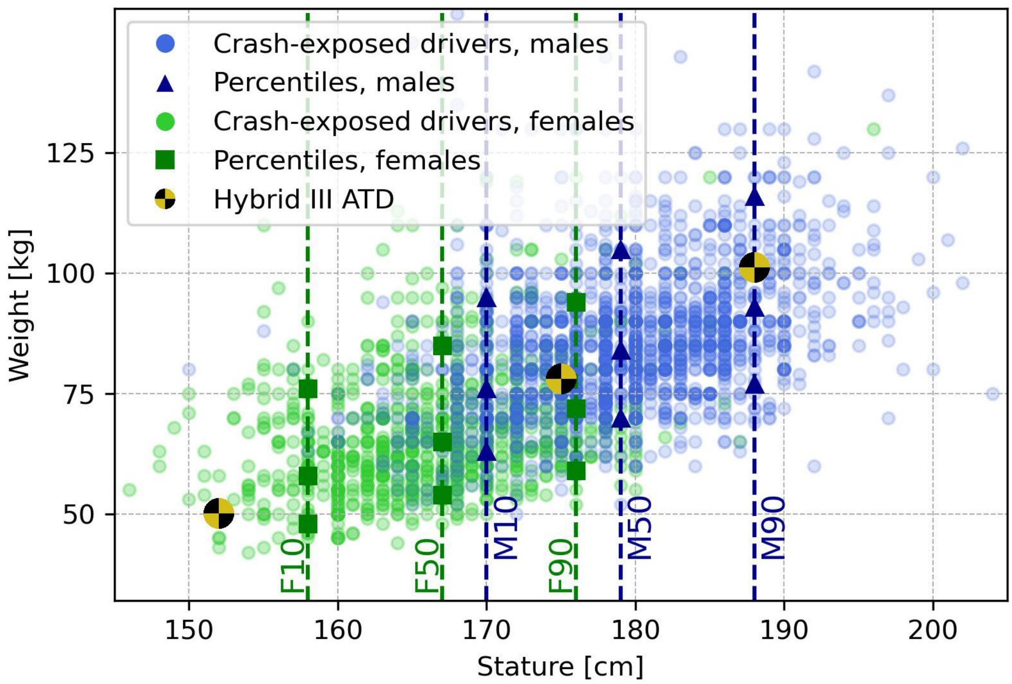

Fig. A1. Weights and statures for crash-exposed females and males, along with the calculated percentiles. ATD statures and weights (Hybrid III 5% female, 50% male, and 95% male) are shown for reference.

To evaluate how well the calculated percentiles represented the population, we assumed that each cell in the 3×3 grid would cover ±4 cm in standing stature and ±5 kg in weight. This assumption was based on engineering judgement of how much such variations could influence occupant protection in a typical crash. No simulations were performed to verify this. Using this range, we calculated what share of the population was covered by each calculated percentile (Table AI and Table AII).

For the simulation study we selected two female and two male weight and stature combinations to represent the population distribution observed in the field data; highlighted in bold in Tables AI and AII. Because of findings from [8-10], where it was shown that occupants who are most frequently exposed to crashes are also those who are most frequently injured, we targeted to have as large coverage as possible while still including a variation in weight and stature. The selected females and males were as follows.

1. Female 10th percentile in stature and 50th in weight (158 cm/58 kg), representing 10.2% of the female dataset. In the study we refer to this as F10.
2. Female 50th percentile in stature and 50th in weight (167 cm/65 kg,) representing 22.3% of the female

dataset. In the study we refer to this as F50.

3. Male 50th percentile in stature and 50th in weight (179 cm/84 kg), representing 17.1% of the male dataset. In the study we refer to this as M50.
4. Male 90th percentile in stature and 50th in weight (188 cm/93 kg), representing 8.3% of the male dataset. In the study we refer to this as M90.

TABLE AI

CALCULATED 10TH, 50TH, AND 90TH PERCENTILES FOR STANDING HEIGHT AND WEIGHT, AND CORRESPONDING COVERAGE (%) ASSUMING ±4 CM AND ±5 KG ACROSS NINE BODY SIZE GROUPS FOR CRASH-EXPOSED FEMALE DRIVERS

Weight (Percentiles)		Stature (Percentiles)			
		10th	50th	90th	BMI
	10th	158 cm, 48 kg	167 cm, 54 kg	176 cm, 59 kg	19
	% of females	4.9%	11.0%	4.5%	
	50th	**158 cm, 58 kg**	**167 cm, 65 kg**	176 cm, 72 kg	23
	% of females	**10.2%**	**22.3%**	5.8%	
	90th	158 cm, 76 kg	167 cm, 85 kg	176 cm, 94 kg	30
	% of females	3.7%	5.7%	1.6%	

TABLE AII

CALCULATED 10TH, 50TH, AND 90TH PERCENTILES FOR STANDING HEIGHT AND WEIGHT, AND CORRESPONDING COVERAGE (%) ASSUMING ±4 CM AND ±5 KG ACROSS NINE BODY SIZE GROUPS FOR CRASH-EXPOSED MALE DRIVERS

Weight (Percentiles)		Stature (Percentiles)			
		10th	50th	90th	BMI
	10th	170 cm, 63 kg	179 cm, 70 kg	188 cm, 77 kg	22
	% of males	3.3%	10.1%	4.6%	
	50th	170 cm, 76 kg	**179 cm, 84 kg**	**188 cm, 93 kg**	26
	% of males	6.9%	**17.1%**	**8.3%**	
	90th	170 cm, 95 kg	179 cm, 105 kg	188 cm, 116 kg	33
	% of males	3.9%	4.4%	1.2%	

Appendix B: Comparison of Hybrid III and SAFER HBM Responses in Two Crash Pulses

We added this appendix to provide a visual understanding of how the restraint system performed in the two crash pulses, 35 km/h and 56 km/h. In addition to what is presented in the main paper, we also show how the more familiar Hybrid III 50th compares with the SAFER HBM version 11 M50 in terms of kinematics and how they load the belt and airbag over time.

By reviewing the curves in Fig. B1 and the sequence images in Fig. B2, the reader can see the differences between the crash pulses and how the pretensioner, load limiter, airbag, and steering system work together in each case. Appendix B provides a more complete picture of how the restraint system behaves in these typical crash pulses.

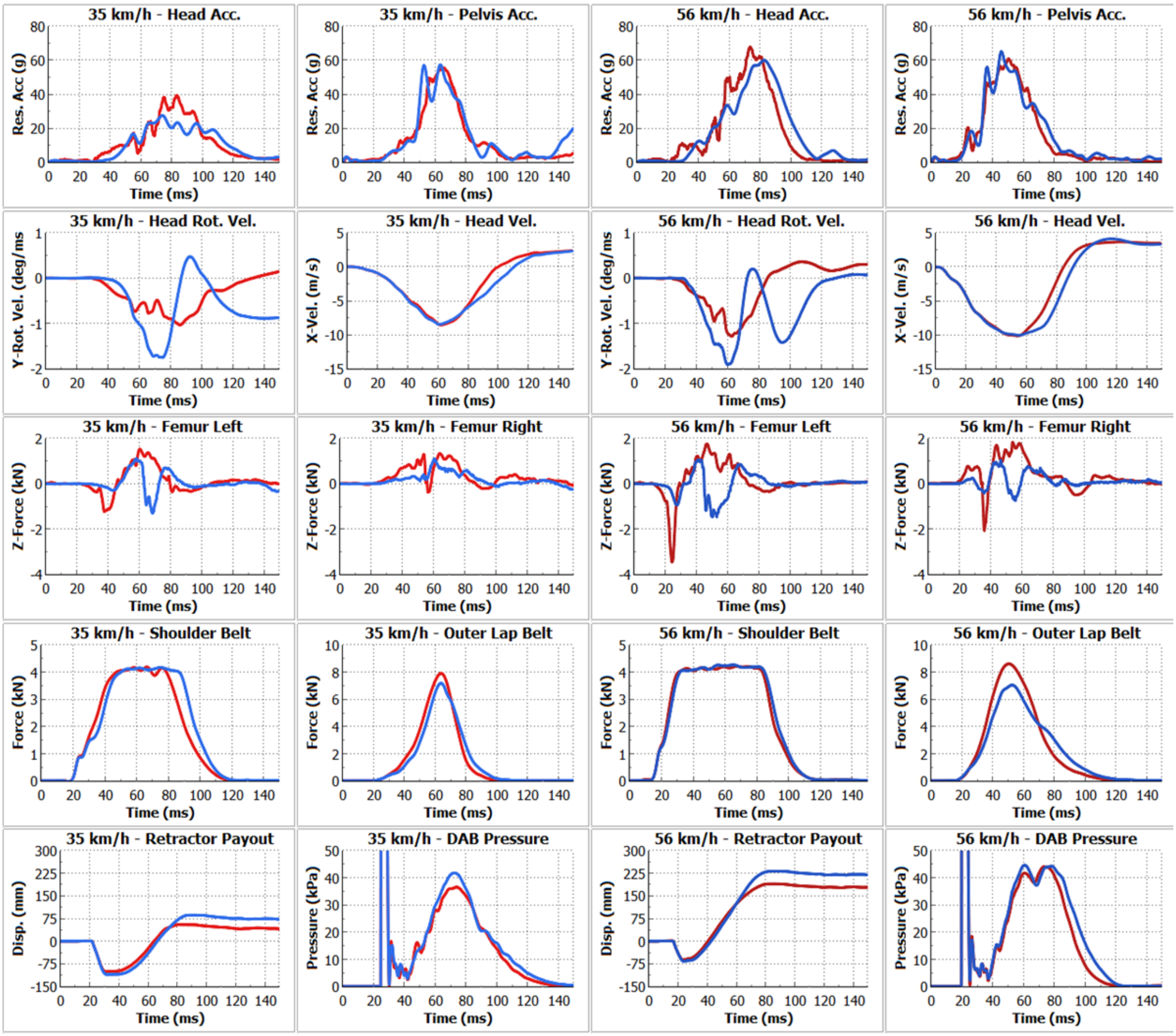

Fig. B1. Simulation comparison of the Hybrid III 50M (red) and SAFER HBM 50M (blue) across the 35 km/h (left two columns) and 56 km/h (right two columns) crash pulses, showing kinematics and restraint-system loads.

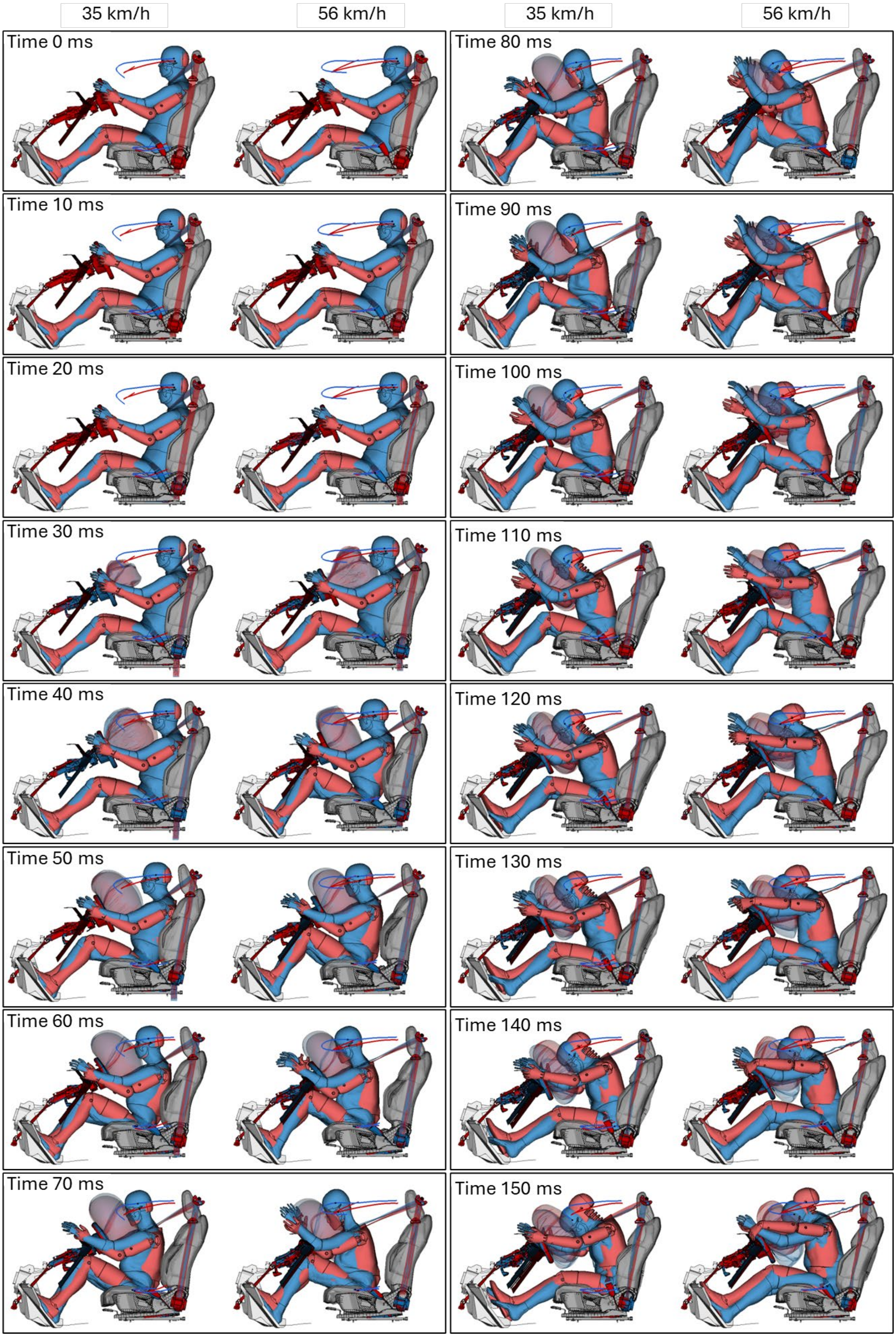

Fig. B2. Visualisation of the Hybrid III 50th (red) and SAFER HBM M50 (blue) kinematics over time, shown at 10 ms intervals, (*left*) 35 km/h and (*right*) 56 km/h.

Appendix C: How Often Different Longitudinal Seat Positions Are Used by Drivers of Different Stature

In this appendix, we present the frequency of longitudinal seat positions chosen by drivers at the 10th, 50th, and 90th stature percentiles for both females (Table CI) and males (Table CII). Longitudinal seat position groups were defined using ±2.5 cm intervals around the GIDAS SWSITZ and ASVKD measurements to reflect the uncertainty and natural spread in real-world seating behaviour. For females, the longitudinal seat positions span from 90 cm to 105 cm, and for males from 95 cm to 110 cm; these ranges were selected as they correspond to the most frequently observed seating positions in the field data. Although these data were not used to set up the simulation matrix, the appendix was added to support future research. Since the field analysis showed no clear injury risk differences across seat positions, the frequency information presented here can help identify which seat positions provide the largest population coverage. This directly supports the Recommendations for Future Research, where population-grounded subsets of field data are needed for more targeted HBM validation.

TABLE CI

CALCULATED FREQUENCY OF LONGITUDINAL SEAT POSITION FOR 10TH, 50TH, AND 90TH PERCENTILE FEMALE DRIVERS

	Stature						
Longitudinal seat position	Range [cm]	10th	% of females	50th	% of females	90th	% of females
	90 ±2.5	158 cm ±4	5.4%	167 cm ±4	8.0%	176 cm ±4	1.7%
	95 ±2.5	158 cm ±4	7.1%	167 cm ±4	15.1%	176 cm ±4	5.6%
	100 ±2.5	158 cm ±4	4.2%	167 cm ±4	11.6%	176 cm ±4	8.8%
	105 ±2.5	158 cm ±4	2.6%	167 cm ±4	5.7%	176 cm ±4	4.2%

TABLE CII

CALCULATED FREQUENCY OF LONGITUDINAL SEAT POSITION FOR 10TH, 50TH, AND 90TH PERCENTILE MALE DRIVERS

	Stature						
Longitudinal seat position	Range [cm]	10th	% of males	50th	% of males	90th	% of males
	95 ±2.5	170 cm ±4	5.4%	179 cm ±4	8.5%	184 cm ±4	2.1%
	100 ±2.5	170 cm ±4	7.6%	179 cm ±4	14.3%	184 cm ±4	5.0%
	105 ±2.5	170 cm ±4	4.2%	179 cm ±4	12.7%	184 cm ±4	9.1%
	110 ±2.5	170 cm ±4	1.4%	179 cm ±4	6.9%	184 cm ±4	6.0%

ERRATUM

Influence of Driver Stature and Seat Position on Injury Risk in Frontal Car Crashes: A Comparative Analysis of Field Data and Human Body Model Simulations

Martin Östling, Daniel Schmidt, Hanna Jeppsson, Linda Erikson, Thomas Lich

After publication, it was discovered that in Fig. 4 the HIII-5F dummy was mistakenly plotted with a stature of 155 cm. The correct stature is 152 cm, as shown in the revised Figure 4 below. It should be noted that the HIII-5F is presented with the correct stature in Fig. 3 and Fig. A1. Although this error does not affect the overall conclusions of the paper, it has a noticeable impact on the visualization when compared with the field data on driver stature and longitudinal seat position. Therefore, we believe it is important to correct the figure to ensure that the published manuscript is as accurate as possible.

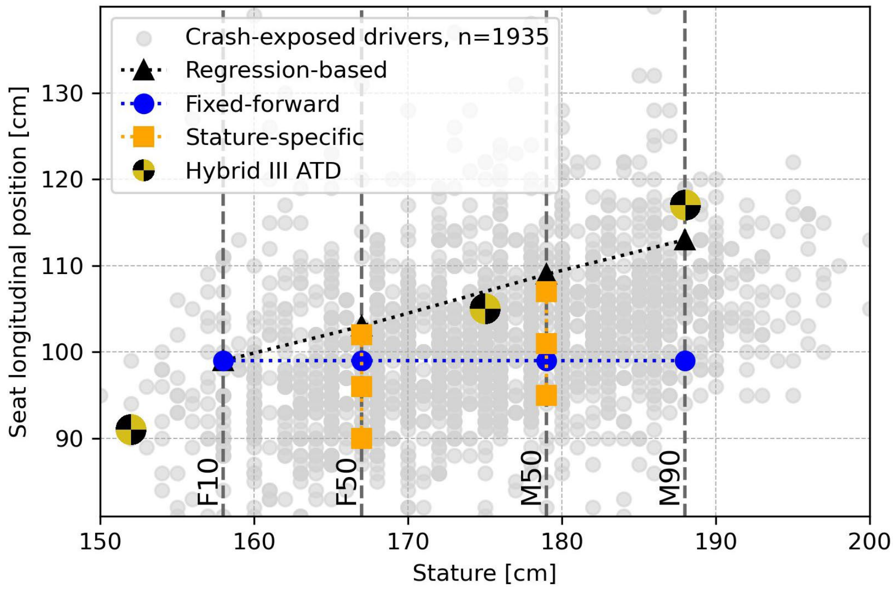

Fig. 4. Stature and longitudinal seat position show a large individual spread with generally more rearward positions for drivers of taller stature. The three different methods for HBM longitudinal seat position are marked with symbols connected for visual guidance with dotted lines. Again, HIII ATDs are marked for reference.

M. Östling (e-mail: martin.ostling@autoliv.com; tel: +46 733 614959) is a System Development Senior Expert, H. Jeppsson is an Accidentology Manager and L. Eriksson is a CAE specialist, all at Autoliv, Sweden. D. Schmidt is a Research Engineer and T. Lich is an Accident Research Senior Expert, both at Robert Bosch Germany.